Ultrasonics 50 (2010) 161–166

Contents lists available at ScienceDirect

Ultrasonics

journal homepage: www.elsevier.com/locate/ultras

Surface acoustic waves in interaction with a dislocation

Agnès Maurel [a], Vincent Pagneux [b], Felipe Barra [c,*], Fernando Lund [c]

[a] Laboratoire Ondes et Acoustique, UMR CNRS 7587, Ecole Supérieure de Physique et Chimie Industrielles, 10 rue Vauquelin, 75005 Paris, France
[b] Laboratoire d'Acoustique de l'Université de Maine, UMR CNRS 6613 Avenue Olivier Messiaen, 72085 Le Mans Cedex 9, France
[c] Departamento de Física and CIMAT, Facultad de Ciencias Físicas y Matemáticas, Universidad de Chile, Casilla 487 – 3, Santiago, Chile

ARTICLE INFO

Article history:
Received 14 July 2009
Received in revised form 7 September 2009
Accepted 14 September 2009
Available online 24 September 2009

PACS:
61.72.Lk
72.10.Fk
11.80.La
81.70.Cv

Keywords:
Surface acoustic waves
Dislocations
Scattering

ABSTRACT

A surface acoustic wave can interact with dislocations that are close to the surface. We characterize this interaction and its manifestations as scattered surface acoustic waves for different orientations with respect to the surface of an edge dislocation. For dislocations that are parallel or perpendicular to the free surface, we present an analytical result for short dislocations with respect to the wave-length that reproduce qualitatively the main features observed for dislocations of various sizes.

1. Introduction

Dislocations determine many properties of metals. For instance, they play a significant role in phenomena such as fatigue [1–3] and in the brittle to ductile transition [4]. However the physics of dislocations is not completely understood. In part, this deficiency is due to the lack of experimental measurements (as opposed to visualizations) concerning dislocations. Dislocations are currently seen through transmission electron microscopy of specially prepared samples [5–7]. It would be of high interest to have quantitative non invasive measurements and ultrasonic probe may provide such quantitative data. In the pursuit of this research program, it seems pertinent to characterize the interaction of surface acoustic waves with dislocations. There are several advantages in this situation: while technically difficult, it is possible to visualize simultaneously the propagation of a surface acoustic wave (SAW) and the response of a nearby dislocation [8,9]. It is also nowadays possible to measure surface deformations with high precision [10]. Such conditions will be difficult to meet in the bulk of the medium. In this respect, SAW measurements seem to provide the best conditions for the development and the validation of acoustic technique.

The interaction of acoustic waves with dislocations was the subject of many studies in the period from the early 1950's to the mid 1980's, with the theory of Granato and Lücke (GL) [11,12] widely accepted as the standard theory to this day [13] due to its success to describe damping, internal friction and modulus change in solids. It is a model based on mean-field concepts where effective quantities such as velocity and attenuation coefficient are obtained. The interaction of a bulk acoustic wave with a single, isolated dislocation is outside the scope of that theory.

In previous works we have studied the interaction of an elastic wave with a single dislocation [14,15]. From this knowledge we were able to study the propagation of an elastic wave in a medium with a random distribution of dislocations [16,17] and in a medium with particular arrangement of dislocation walls for application to propagation in polycrystals [18–20]. This description takes fully into account the vectorial character of the elastic waves and of the dislocations in the solid. Moreover, we showed that after some simplifications appropriate to recover scalar quantities, the GL theory follows from our formulation [17]. Later we described the physics of the interaction of a single dislocation with a SAW [21]. Here we dwell on this topic and study the scattering amplitudes for dislocations with different orientations with respect to the surface and provide an analytical expression valid in the long wave-length limit for the scattering amplitude of dislocations

* Corresponding author. Tel.: +56 2 6784350.
E-mail address: fbarra@dfi.uchile.cl (F. Barra).

0041-624X/$ - see front matter © 2009 Elsevier B.V. All rights reserved.
doi:10.1016/j.ultras.2009.09.020

perpendicular and parallel to the surface. The formulas provide an understanding of the main dependence of scattering amplitudes on the length and depth of the dislocation.

2. Theoretical framework

We consider a single dislocation segment in an isotropic elastic medium of density ρ and Lamé constants μ and λ such that longitudinal waves propagate with speeds $c_L = \sqrt{(\lambda+2\mu)/\rho}$ and transversal with $c_T = \sqrt{\mu/\rho}$. The dislocation is represented by a line $\mathbf{X}(s,t)$ in the three dimensional space parametrized by the arc-length s and time t.

The equation of motion for the dislocation consists of four terms, one that takes into account the inertia of the dislocation, another one the damping, the third takes into account the tension of the dislocation line and the last, the force that acts on the dislocation:

$$m\frac{\partial^2 X_i}{\partial t^2} + B\frac{\partial X_i}{\partial t} - \Gamma\frac{\partial^2 X_i}{\partial s^2} = F_i. \tag{1}$$

All but the second term, are derived from the variational principle [22] that rules the continuous theory of elasticity. Explicit expressions for the mass m and the line tension Γ are

$$m = \frac{\rho b^2}{4\pi}(1+\gamma^{-4})\ln\left(\frac{\delta}{\delta_0}\right)$$
$$\Gamma = \frac{\rho b^2 c_T^2}{4\pi}(1-\gamma^{-2})\ln\left(\frac{\delta}{\delta_0}\right) \tag{2}$$

where $\gamma = c_L/c_T$ and b the modulus of the Burgers vector $\mathbf{b}$. These quantities are obtained in terms of two cutoff lengths: the small one δ_0 is used to isolate the core of the dislocation where nonlinear deformations are important and the large one δ represents the size of the system or the distance to another defect.

In Eq. (1), the second term, proportional to the drag coefficient B is introduced phenomenologically. Its precise value is difficult to compute and measure [23] and it is an example of a quantity that could be measured with an acoustic tool.

The force F_i is the classical Peach–Koehler force

$$F_k(\mathbf{x},t) = \epsilon_{kjm}\tau_m b_i \sigma_{ij}(\mathbf{x},t) \tag{3}$$

when the velocities are small in comparison with the speed of wave propagation, as it will be the case in the sequel. ϵ_{kjm} is the completely antisymmetric tensor of rank three, τ_m is a unit tangent along the dislocation line, and $\sigma_{ij}(\mathbf{x},t)$ is the external stress which, in Eq. (1), is evaluated at the dislocation position, $\mathbf{x} = \mathbf{X}(s,t)$.

Under the Born approximation, the scattering of an elastic wave with a dislocation is understood in two steps. First a wave hits a dislocation and its stress forces the dislocation through the Peach–Koehler force. The dislocation will move and emit elastic waves. Before turning to this emission let us mention that we are neglecting the scattering that the wave could experience by crossing the core of the dislocation where strong deformations of the crystal exist. This mechanism should be important only for waves with small wave-length like thermal waves.

Once the dislocation moves, it will generate waves. In fact, the dislocation motion enters as a boundary condition for the wave equation that can also be represented as a source term. We explain this in more detail below.

Neglecting the pre-stress due to the dislocation at rest, the wave is described by the displacement vector $\mathbf{u}$ that is a solution of the wave equation

$$\rho\frac{\partial^2}{\partial t^2}u_i(\mathbf{x},t) - c_{ijkl}\frac{\partial^2}{\partial x_j \partial x_l}u_k(\mathbf{x},t) = 0,$$

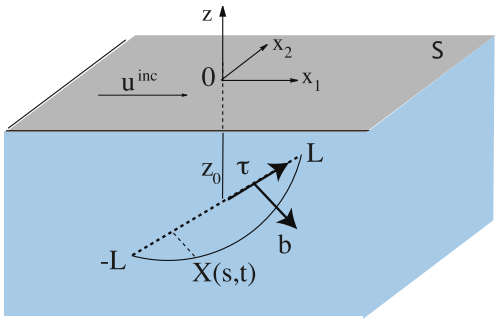

Fig. 1. A subsurface dislocation segment lying in a semi-infinite half space with a stress-free boundary is excited by a surface Rayleigh wave. It responds by oscillating, and reradiating. At the free surface, these secondary waves will interfere with the incident wave [21].

where $c_{ijkl} = \lambda\delta_{ij}\delta_{kl} + \mu(\delta_{ik}\delta_{jl} + \delta_{il}\delta_{jk})$ and with the following two boundary conditions: (1) on one hand, the displacement has a discontinuity equal to the Burgers vector when crossing a time-dependent surface $S(t)$ whose contour is the moving dislocation line $\mathscr{L}(t)$: $[u_i]_{S(t)} = b_i$, on the other hand the stress is single valued: $[c_{ijkl}(\partial u_l/\partial x_k)n_j]_{S(t)} = 0$; (2) the normal stress vanishes at the free surface S, defined by $z = 0$: $[c_{ijkl}(\partial u_l/\partial x_k)n_j]_S = 0$. This last condition is absent in the infinite medium.

The solution for the time derivative of the wave displacement $\mathbf{v} = \partial\mathbf{u}/\partial t$, the particle velocity, can be written in the form of a convolution with a source localized along the loop, an expression first given in [24], see also [16]:

$$v_i^s(\mathbf{x},t) = -\epsilon_{jnh}c_{pjkl}\int_{\mathscr{L}}\int dt'ds\; b_p\dot{X}_n(s,t')\tau_h\frac{\partial}{\partial X_l}G^0_{ik}[\mathbf{x},\mathbf{X}(s,t');t-t'], \tag{4}$$

where we denote $\dot{X} \equiv \partial X/\partial t$ and G^0 is the Green function of the half space with a free surface.[1] This expression is a solution of

$$\rho\frac{\partial^2 v_i}{\partial t^2} - c_{ijkl}\frac{\partial^2 v_k}{\partial x_j \partial x_l} = s_i \tag{5}$$

where the source term s_i is

$$s_i(\mathbf{x},t) = c_{ijkl}\epsilon_{mnk}\int_{\mathscr{L}} ds\;\dot{X}_m(s,t)\tau_n b_l\frac{\partial}{\partial x_j}\delta(\mathbf{x}-\mathbf{X}(s,t)).$$

We end this section with the remark that from a theoretical point of view, the results of this section holds just as well for a whole space as for half space, the difference being that G^0_{im} is now the impulse response function of an elastic half-space with a stress-free boundary instead of the response function of the whole space.

3. Pinned dislocation segment in a half space

The physical situation we consider is as follows (see Fig. 1): an incident Rayleigh wave, with angular frequency ω, is launched at the free surface of a semi-infinite elastic medium containing an isolated edge dislocation line. The line can have any direction but we assume it does not touch the free surface. It is assumed that the dislocation can be represented by a straight segment of length $2L$ pinned at its extremities so that in equilibrium $\mathbf{X}(s) = (0,0,z_0) + s\boldsymbol{\tau}$ $(-L \leqslant s \leqslant L)$ and when moving it must satisfy the boundary conditions $X_k(\pm L,t) = 0$. Neglecting dislocation climb, the motion of the dislocation occurs along the direction of the Burgers vector (gliding edge dislocation).

[1] G^0_{im} satisfies an equation similar to Eq. (5) but with right-hand side given by $\delta_{im}\delta(t-t')\delta(\mathbf{x}-\mathbf{x}')$. See [21] for details.

We denote $\mathbf{t}$ the glide direction, with $\mathbf{b} = b\mathbf{t}$, $\boldsymbol{\tau}$ the unit tangent along the dislocation line, and $\mathbf{n} \equiv \boldsymbol{\tau} \times \mathbf{t}$. We suppose that the dislocation oscillates with an amplitude which is small compared to the wave-length, so that its time dependent position can be replaced by the static, equilibrium, position $\mathbf{X}(s,t) \simeq \mathbf{X}(s)$ in the expression (4). Also, for a gliding motion, $\dot{X}_n(s,t) = \dot{X}(s,t)t_n$ and we use $\epsilon_{jnh}t_n\tau_h = -n_j$. In the frequency domain ($e^{-i\omega t}$), Eq. (4) becomes for the vertical component

$$v_z^s(\mathbf{x},\omega) = -i\omega\mu b \int_{\mathscr{S}} ds\, X(s,\omega)\mathsf{M}_{lk}\partial_{X_l}G^0_{3k}[\mathbf{x},\mathbf{X}(s);\omega], \tag{6}$$

where $\mathsf{M} \equiv \mathbf{n}\,{}^t\mathbf{t} + \mathbf{t}\,{}^t\mathbf{n}$ and $c_{ijkl}t_in_j = \mu\mathsf{M}_{lk}$. Note that $\mathbf{u}(\mathbf{x},\omega) = i\mathbf{v}(\mathbf{x},\omega)/\omega$. We consider only the vertical component of $\mathbf{v}$ at the surface because it is a quantity accessible to experiments. v_z^s is the scattered wave because it is the wave emitted in reaction to the incident wave. We treat this scattering problem in the Born approximation, this means that in solving the equation of motion for $X(s,\omega)$, we only consider the force produced by the incident Rayleigh wave. This is addressed in the next subsection. The determination of $\partial_{X_l}G^0_{3k}(\mathbf{x},\mathbf{X};\omega)$ in Eq. (6) is more involved and was considered in detail in [21].

3.1. The motion of the dislocation line: $X(s,\omega)$

Let us find the response of the dislocation to the surface wave. This is given by the solution of Eq. (1) with the Peach–Koehler force at its right-hand side computed from the resolved shear stress generated by the incoming surface wave at the position of the dislocation. The incoming wave is a surface (Rayleigh) wave, whose wave vector is $k_R \equiv \omega/c_R$, where $c_R \equiv \zeta c_T$, $\zeta \sim 0.9$ being the zero of the Rayleigh polynomial $P(\zeta) = \zeta^6 - 8\zeta^4 + 8\zeta^2(3 - 2/\gamma^2) - 16(1 - 1/\gamma^2)$. This wave is not dispersive, and has an elliptical polarization, a combination of the longitudinal and transverse perpendicular to the free surface [25]. For a wave propagating along the x_1-direction the displacements associated to this wave are

$$\begin{aligned} u_1^{inc}(\mathbf{x},\omega) &= (k_R A e^{\nu_L z} + \nu_T e^{\nu_T z})e^{ik_R x_1}, \\ u_z^{inc}(\mathbf{x},\omega) &= -i(\nu_L A e^{\nu_L z} + k_R e^{\nu_T z})e^{ik_R x_1}, \end{aligned} \tag{7}$$

where $A \equiv -2\sqrt{1-\zeta^2}/(2-\zeta^2)$, and $\nu_{L,T} \equiv \sqrt{k_R^2 - k_{L,T}^2} > 0$ ($k_{L,T} \equiv \omega/c_{L,T}$).

Note that the deformation induced by the surface wave increases from the surface to the interior of the medium, reaches a maximum and then decreases to zero (see Fig. 2). The deformation in the x_1 direction vanishes for $k_R z_1^{zero} = 4\sqrt{1-\zeta^2}/\zeta^4 \ln[1-\zeta^2/2]$ and reaches its maximum at $k_R z_1^m = -4\sqrt{1-\zeta^2}/\zeta^4 \ln[(1-\zeta^2/2)/(1-\zeta^2)]$. The deformation in the z direction has it maximum at $k_R z_z^m = -4\sqrt{1-\zeta^2}/\zeta^4 \ln[(1-\zeta^2/2)^3/(1-\zeta^2)]$ (where we have used $2\nu_L k_R A = k_T^2 - 2k_R^2$ or equivalently $A = (\zeta^2-2)/2\sqrt{1-\zeta^2/\gamma^2}$). Note that these values, depend only on ζ or equivalently only on γ, which characterize the material. For positive Poisson's ratio $\nu = (\gamma^2-2)/2(\gamma^2-1)$, we get $k_R z_1^{zero} \sim -1$, $k_R z_1^m \sim -3$ and $k_R z_z^m \in [-1, 0]$. Finally, these values, in addition to the depth of the dislocation and the orientation of the glide plane, will determine the sensitivity of the dislocation to the wave and therefore the scattering strength as we show later.

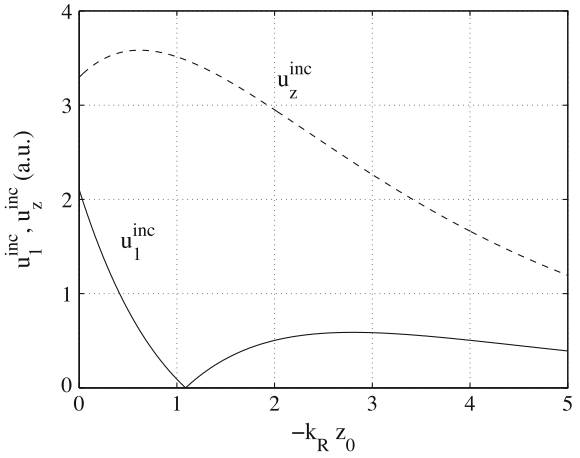

Fig. 2. The vertical u_z^{inc} and longitudinal u_1^{inc} displacements associated to the SAW (here, with $\gamma = 1.9$).

When Eq. (1) is projected to the glide plane, the projected Peach–Koehler force $\mathbf{F} = F\mathbf{t}$ produced by the incident wave at the dislocation position $\mathbf{X}(s,\omega)$ is given by $F = \mu b\mathsf{M}_{lk}\partial_{x_l}u_k^{inc} = \mu b[2n_1t_1\partial_{x_1}u_1^{inc} + 2n_3t_3\partial_z u_z^{inc} + (n_1t_3 + n_3t_1)(\partial_{x_1}u_z^{inc} + \partial_z u_1^{inc})]$. In the frequency domain, we have to solve

$$\begin{aligned} X''(s,\omega) + K^2X(s,\omega) &= -\frac{1}{\Gamma}F(s,\omega) \\ &= -(C_L(\omega)e^{\alpha_L s} + C_T(\omega)e^{\alpha_T s}), \end{aligned} \tag{8}$$

where X'' denotes $\partial^2X/\partial s^2$, $K \equiv \sqrt{(m\omega^2 + iB\omega)/\Gamma}$,

$$\begin{aligned} C_L &\equiv 2\tfrac{\mu b}{\Gamma}Ae^{\nu_L z}\left[i\left(n_1t_1k_R^2 - n_3t_3\nu_L^2\right) + (n_1t_3 + n_3t_1)k_R\nu_L\right], \\ C_T &\equiv \tfrac{\mu b}{\Gamma}e^{\nu_T z}\left[2i(n_1t_1 - n_3t_3)k_R\nu_T + (n_1t_3 + n_3t_1)(k_R^2 + \nu_T^2)\right], \end{aligned} \tag{9}$$

and $\alpha_{L,T} \equiv \nu_{L,T}\tau_3 + ik_R\tau_1$. In Eq. (9) we used $z = z_0 + s\tau_3$, the depth of the dislocation point whose parameter is s. The solution is

$$\begin{aligned} X(s,\omega) = &\frac{C_L}{\alpha_L^2 + K^2}\left[e^{\alpha_L s} - \frac{\cosh\alpha_L L}{\cos KL}\cos Ks - \frac{\sinh\alpha_L L}{\sin KL}\sin Ks\right] \\ &+ \frac{C_T}{\alpha_T^2 + K^2}\left[e^{\alpha_T s} - \frac{\cosh\alpha_T L}{\cos KL}\cos Ks - \frac{\sinh\alpha_T L}{\sin KL}\sin Ks\right]. \end{aligned} \tag{10}$$

The functions C_L and C_T that depend on the direction of the glide plane determine the amplitude of the dislocation motion. These functions reflect in the amplitude of dislocation motion the fact that the incident wave has a maximum at some depth. We discuss this later in the light of numerical results.

3.2. The long wave-length limit: an analytical expression for the scattered wave

If the wave-length is large compared to the length of the dislocation i.e., $k_R L \ll 1$, the term that depends on the Green tensor is approximately a constant on the length scale of the dislocation line and can be taken out of the integral in Eq. (6)

$$v_z(\mathbf{x},\omega) = -i\omega\mu b\mathsf{M}_{lk}\partial_{x_l}G^0_{3k}(\mathbf{x},\mathbf{X}_0,\omega)\int ds X(s,\omega), \tag{11}$$

For a vertical dislocation line ($\boldsymbol{\tau} = (0,0,1)$, perpendicular to the free surface), the Burgers vector is on a plane parallel to the free surface with an orientation α with respect to x_2 i.e., $\mathbf{t} = (-\sin\alpha, \cos\alpha, 0)$ in the $(x_1,\ x_2)$ plane. The term with the gradient reduces to

$$M_{lk}\partial_{x_l}G^0_{3k}(\mathbf{x},\mathbf{X}_0,\omega) = \frac{1}{2\pi\mu}\sin 2(\theta - \alpha)I_{f_2}(r,\mathbf{X}_0), \tag{12}$$

with $\mathbf{x} = (r,\theta,0)$ in cylindrical coordinates and

$$I_{f_2}(r,\mathbf{X}_0) \equiv \int_0^{+\infty} dk\ k^3J_2(kr)f(k,z_0), \tag{13}$$

where $f(k,z_0)=\left[\left(k_T^2-2k^2\right)e^{\xi_L z_0}+2\xi_L\xi_T e^{\xi_T z_0}\right]/F(k)$ with $F(k)\equiv(k_T^2-2k^2)^2-4k^2\xi_L\xi_T$, which vanishes at $k=k_R$ and $\xi_{L,T}\equiv\sqrt{k^2-k_{L,T}^2}$. As a complex function of k, $f(k,z_0)$ has a pole at k_R and other singularities such as branch points at $\pm k_L,\pm k_T$ that forbid an explicit integration for I_{f_2}; however, it is possible to find an analytical expression valid in the far field $k_R r\gg 1$ limit. With this purpose we rewrite I_{f_2} as

$$I_{f_2}(r)=\frac{1}{2}\int_{-\infty}^{+\infty}dk\ k^3H_2^{(1)}(kr)f(k,z_0)$$

where we have used the fact that $f(k,z_0)$ is an even function of k and the relation $J_2(kr)=\left[H_2^{(1)}(kr)-H_2^{(1)}(-kr)\right]/2$ between the Bessel function of the first kind J_2 and the Hankel function of first kind $H_2^{(1)}$. In the far field $k_R r\gg 1$, the contribution of the Rayleigh pole is expected to be dominant [26] and thus, neglecting other singularities of $f(k,z_0)$ Cauchy residue theorem allows us to obtain the following analytical expression

$$I_{f_2}(r,\mathbf{X}_0)\simeq i\pi\frac{k_R^3H_2^{(1)}(k_Rr)}{F'(k_R)}\left(\left(k_T^2-2k_R^2\right)e^{v_Lz_0}+2v_Lv_Te^{v_Tz_0}\right),\tag{14}$$

with $F'(k_R)=-8k_R\left(k_T^2-2k_R^2\right)-4k_R\left[2v_L^2v_T^2+k_R^2\left(v_L^2+v_T^2\right)\right]/(v_Lv_T)$.

In the long wave-length limit, the motion of the dislocation also simplifies because the Peach–Koehler force that acts on the dislocation is a constant along the line given by

$$\begin{aligned}F&=\mu b\ \mathrm{M}_{lk}\partial_l u_k^{inc}(\mathbf{X}_0,\omega)=\mu b\ \sin2\alpha\partial_{x_1}u_1^{inc}(\mathbf{X}_0,\omega)\\&=i\mu bk_R(k_RAe^{v_Lz_0}+v_Te^{v_Tz_0}),\end{aligned}\tag{15}$$

solving the equation of motion for the dislocation under this force the following expression is obtained

$$X(s,\omega)=-\mu b\frac{i}{\Gamma K^2}k_R(k_RAe^{v_Lz_0}+v_Te^{v_Tz_0})\left(1-\frac{\cos Ks}{\cos KL}\right).\tag{16}$$

with K defined after Eq. (8). Substituting Eq. (14) in Eq. (12) and plugging the result in Eq. (11) together with the integral of Eq. (16) we obtain our analytical approximation for the scattered wave $v_z^{s\perp}$ by a dislocation segment perpendicular to the free surface

$$\begin{aligned}v_z^{s\perp}(\mathbf{x},\omega)=&-\omega k_R\frac{\mu b^2}{mc_T^2}\frac{m\omega^2}{\Gamma K^2}\sin2\alpha\sin2(\theta-\alpha)\\&f_1^{\perp}(k_Rz_0)\,f_2(L)\,H_2^{(1)}(k_Rr),\end{aligned}\tag{17}$$

$$\begin{aligned}&f_1^{\perp}(k_Rz_0)\equiv\tfrac{-i(\zeta^2-2)^2}{2\zeta^2\sqrt{1-\zeta^2}h(\zeta)}\left[e^{v_Lz_0}+(\zeta^2/2-1)e^{v_Tz_0}\right]^2\\&f_2(L)\equiv k_RL\left(1-\tfrac{\tan KL}{KL}\right).\end{aligned}\tag{18}$$

Here $h(\zeta)\equiv2(4-\zeta^4)-(2-\zeta^2)^2/(1-\zeta^2)-16(1-\zeta^2)/(2-\zeta^2)^2\sim\ -3$ for $\zeta\sim0.9$. Note that the scattered wave amplitude $v_z^{s\perp}$ is proportional to ωk_R because $u^{\mathrm{inc}}\propto k_R$. The coefficient $\mu b^2/mc_T^2$ is of order one and $\Gamma K^2/m\omega^2=1+iB/(m\omega)$ depends on the drag coefficient.

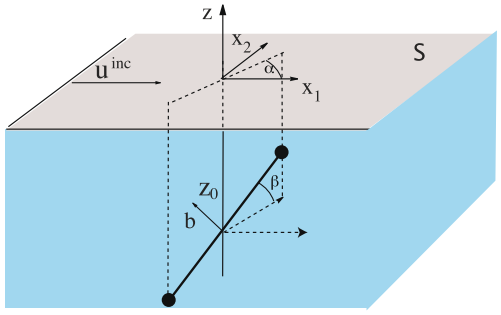

Fig. 3. The configuration of the dislocation and the angles that define its orientation. The dislocation line has an angle β with the (x_1,x_2)-plane and the Burgers vector lies in the (x_1,x_2) plane, forming an angle α with the x_2-axis.

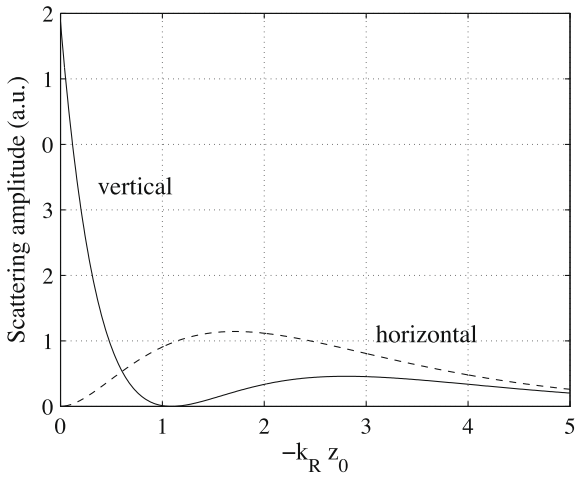

Fig. 4. The scattered amplitude for a vertical and horizontal dislocation excited by a SAW (here, with $\gamma=1.9$).

A similar calculation for a small horizontal dislocation line ($\beta=0$ with the notations of Fig. 3), whose glide plane is parallel to the free surface, and $(\boldsymbol{\tau},\mathbf{t})$ is deduced from $(\mathbf{x}_1,\mathbf{x}_2)$ by a rotation of angle α, gives the scattered wave $v_z^{s\parallel}$

$$v_z^{s\parallel}(\mathbf{x},\omega)=-\omega k_R\frac{\mu b^2}{mc_T^2}\frac{m\omega^2}{\Gamma K^2}\sin\alpha\ \sin(\theta-\alpha)f_1^{\parallel}(k_Rz_0)\,f_2(L)\,H_1^{(1)}(k_Rr),\tag{19}$$

where

$$f_1^{\parallel}(k_Rz_0)\equiv\frac{(\zeta^2-2)^4}{2\zeta^2\sqrt{1-\zeta^2}h(\zeta)}[e^{v_Lz_0}-e^{v_Tz_0}]^2.\tag{20}$$

This last result, without the detailed derivation was presented in [21].

These expressions for the scattered wave by a vertical ($\beta=\pi/2$ with the notations of Fig. 3) and horizontal ($\beta=0$) dislocations are *a priori* valid only in the far field but, as shown in [21] for the vertical case, when $|k_Rz_0|$ is small enough, that is, when the dislocation line is near the free surface, they give a reasonable approximation of the overall field.

In Fig. 4 we plot the scattering amplitude for both cases as a function of z_0. This dependence appears through the functions $f_1^{\parallel}$ and $f_1^{\perp}$. We observe that, for an horizontal dislocation, the scattering amplitude is maximum when the dislocation is at a depth near $1.5/k_R$. For a vertical dislocation, the scattering amplitude vanishes at a depth near $1/k_R$ and reaches its maximum near $3/k_R$. These values are determined mainly by the dependence on the depth of the force acting over the dislocation which in turns depends on the dependence on the depth of the incident wave. In Fig. 2 we see that the intensity of the incident wave has a maximum at depth near $2.5/k_R$ for the horizontal displacement. Because the glide plane is parallel to the surface it is expected that this component of the incident wave is more relevant than the horizontal.

The scattering strength increases with increasing L. For small L, this dependence is L^3 as predicted by the function f_2 given in Eq. (18) and departs from this behavior for large L. A similar trend is observed in larger dislocations [21].

A very interesting difference between perpendicular and vertical dislocation is that the diffraction pattern of the former is quadripolar while the later is dipolar. We have computed the pattern of the scattered wave to inspect the influence of the orientation of the

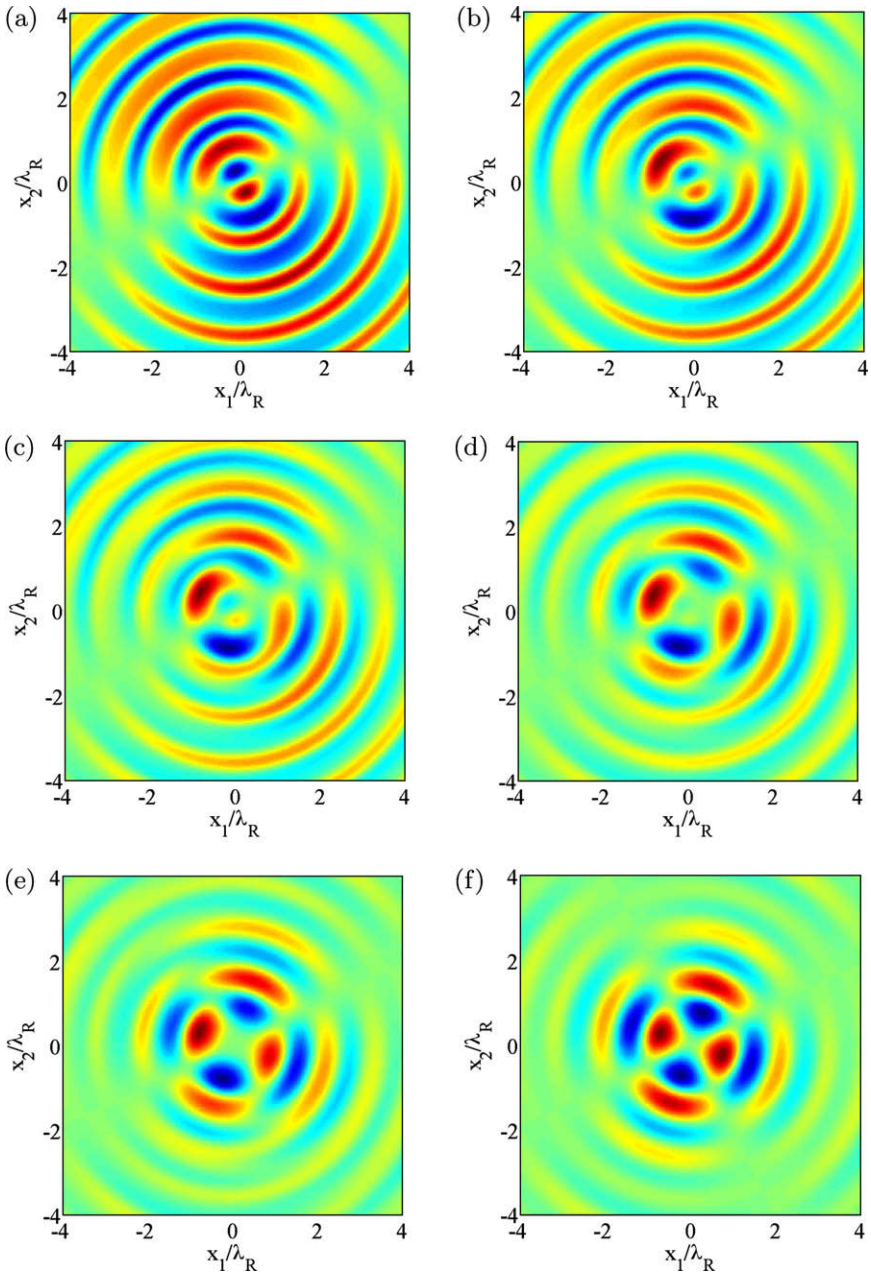

Fig. 5. Pattern of the scattered wave, numerically calculated for $L = \lambda_R/10$, $z_0 = -\lambda_R$. The Burgers vector is along the direction $\mathbf{t} = (-\sin\alpha, \cos\alpha, 0)$ with $\alpha = \pi/7$, the dislocation line is along the direction $\tau = (\cos\beta\cos\alpha, \cos\beta\sin\alpha, \sin\beta)$ with varying β value. (a) $\beta = 0$, the dislocation line is parallel to the free surface, (b) $\beta = \pi/4$, (c) $\beta = \pi/3$, (d) $\beta = 2\pi/5$, (e) $\beta = 9\pi/20$, (f) $\beta = \pi/2$ the dislocation line is perpendicular to the free surface.

dislocation line in the transition from dipolar for an horizontal dislocation to quadrupolar for a vertical one. The dislocation line is along $\tau = (\cos\beta\cos\alpha, \cos\beta\sin\alpha, \sin\beta)$ and the Burgers vector $\mathbf{t} = (-\sin\alpha, \cos\alpha, 0)$ with varying β value and $\alpha = \pi/7$. Fig. 5 shows the result for varying β value.

4. Conclusions

The SAW diffraction pattern induced by a subsurface dislocation depends on several parameters such as depth of the dislocation, orientation, Burgers vector and drag coefficient B. We have studied here mainly the dependence on their orientation, showing that short dislocation segments have a dipolar radiation for horizontal dislocations and quadrupolar for vertical dislocations. For large dislocations segments the analysis can be performed only numerically and this was considered in [21] for dislocations parallel to the surface.

As we noticed previously the formalism of wave dislocation interaction applies to bulk waves and to surface waves interacting with dislocations. The difference is mainly due to the response function that should be used. Dynamical observations of dislocation motion on a free surface can help in the task of increasing the deformations produced by dislocations to levels accessible to experiments. For instance as shown elsewhere [27], the vertical displacement generated by an infinite, straight, dislocation placed at a depth h below the free surface of a semi-infinite medium, that oscillates along its glide plane with frequency ω of the order of the GHz could be as large as 50 times the displacement induced on a plane at a distance h for a static dislocation in the bulk.

Acknowledgments

This work has been supported by FONDAP Grant No. 11980002.

References

[1] S. Kenderian, T.P. Berndt Jr., R.E. Green, B.B. Djordjevic, Ultrasonic monitoring of dislocations during fatigue of pearlitic rail steel, Mater. Sci. Eng. A 348 (2003) 90–99.
[2] S. Kenderian, T.P. Berndt Jr., R.E. Green, B.B. Djordjevic, Ultrasonic attenuation and velocity in pearlitic rail steel during fatigue using longitudinal wave probing, J. Test. Eval. 31 (2003) 98–105.
[3] S. Suresh, Fatigue of Materials, second ed., Cambridge University Press, 1998.
[4] S.G. Roberts, in: J. Lepinoux et al. (Eds.), Multiscale Phenomena in Plasticity, Kluwer, 2000.
[5] X. Xu, S.P. Beckman, P. Specht, E.R. Weber, D.C. Chrzan, R.P. Erni, I. Arslan, N. Browning, A. Bleloch, C. Kisielowski, Distortion and segregation in a dislocation core region at atomic resolution, Phys. Rev. Lett. 95 (2005) 145501.
[6] K. Arakawa, M. Hatakana, E. Kuramoto, K. Ono, H. Mori, Changes in the Burgers vector of perfect dislocation loops without contact with the external dislocations, Phys. Rev. Lett. 96 (2006) 125506.
[7] I.A. Robertson, P.J. Ferreira, G. Dehm, R. Hull, E.A. Stach, Visualizing the behavior of dislocations – seeing is believing, MRS Bull. 33 (2008) 122–131.
[8] D. Shilo, E. Zolotoyabko, Visualization of surface acoustic wave scattering by dislocations, Ultrasonics 40 (2002) 921–925.
[9] D. Shilo, E. Zolotoyabko, Stroboscopic X-ray imaging of vibrating dislocations excited by 0.58 GHz phonons, Phys. Rev. Lett. 91 (2003) 115506.
[10] D.H. Hurley, O.B. Wright, O. Matsuda, T. Suzuki, S. Tamura, Y. Sugawara, Time-resolved surface acoustic wave propagation across a single grain boundary, Phys. Rev. B 73 (2006) 125403.
[11] A.V. Granato, K. Lücke, Theory of mechanical damping due to dislocations, J. Appl. Phys. 27 (1956) 583.
[12] A.V. Granato, K. Lücke, Application of dislocation theory to internal friction phenomena at high frequencies, J. Appl. Phys. 27 (1956) 789.
[13] A.V. Granato, K. Lücke, in: W.P. Mason (Ed.), Physical Acoustics, vol. 4A, Academic, 1966.
[14] A. Maurel, J.-F. Mercier, F. Lund, Scattering of an elastic wave by a single dislocation, J. Acoust. Soc. Am. 115 (6) (2004) 2773–2780.
[15] A. Maurel, V. Pagneux, F. Barra, F. Lund, Interaction between an elastic wave and a single pinned dislocation, Phys. Rev. B 72 (2005) 174110.
[16] A. Maurel, J.-F. Mercier, F. Lund, Elastic wave propagation through a random array of dislocations, Phys. Rev. B 70 (2004) 024303.
[17] A. Maurel, V. Pagneux, F. Barra, F. Lund, Wave propagation through a random array of pinned dislocations: velocity change and attenuation in a generalized Granato and Lücke theory, Phys. Rev. B 72 (2005) 174111.
[18] A. Maurel, V. Pagneux, D. Boyer, F. Lund, Elastic wave propagation through a distribution of dislocations, Mater. Sci. Eng. A 400 (2005) 222–225.
[19] A. Maurel, V. Pagneux, D. Boyer, F. Lund, Propagation of elastic waves through polycrystals: the effect of scattering from dislocation arrays, Proc. Roy. Soc. Lond. A 462 (2073) (2006) 2607–2623.
[20] A. Maurel, V. Pagneux, F. Barra, F. Lund, Multiple scattering from assemblies of dislocation walls in 3D. Application to propagation in polycrystals, J. Acoust. Soc. Am. 121 (6) (2007) 3418–3431.
[21] A. Maurel, V. Pagneux, F. Barra, F. Lund, Interaction of a surface wave with a dislocation, Phys. Rev. B 75 (2007) 224112.
[22] F. Lund, Response of a stringlike dislocation loop to an external stress, J. Mater. Res. 3 (1988) 280.
[23] E.M. Nadgornyi, Dislocation dynamics and mechanical properties of crystals, Prog. Mater. Sci. 31 (1988) 1.
[24] T. Mura, Continuous distribution of moving dislocations, Philos. Mag. 8 (1963) 843.
[25] L.D. Landau, E.M. Lifshitz, Theory of Elasticity, second ed., Pergamon, 1981.
[26] J.D. Achenbach, Calculation of surface wave motions due to a subsurface point force: an application of elastodynamic reciprocity, J. Acoust. Soc. Am. 107 (2000) 1892.
[27] A. Maurel, V. Pagneux, F. Barra, F. Lund, Phys. Rev. B, accepted for publication.